

## **Experimental demonstration of time-irreversible, self-ordering evolution processes in macroscopic quantum systems.**

**A. Titov, I. Malinovsky<sup>†</sup>.**

Physics Department, Yeditepe University, Istanbul, Turkey; [atitov@yeditepe.edu.tr](mailto:atitov@yeditepe.edu.tr).

<sup>†</sup>National Metrology Institute, INMETRO, Rio de Janeiro, Brazil, [laint@inmetro.gov.br](mailto:laint@inmetro.gov.br).

**Abstract:** Using the recently developed method, which presents the combination of the modulation technique with synchronous differential thermal measurements, we have demonstrated experimentally the existence of thermal surface energy (TSE) in metallic blocks with signal-to-noise ratio of several thousands. The TSE arises when there are changes of energy and momentum of the coupled field-particle system inside the material artifact, produced by the irradiation of the artifact surface by an external EM field. It is shown that the magnitude of TSE and the direction of its increase are defined by the Poynting vector of the external field. The fundamental features of the TSE - the lack of symmetry in space and the irreversible character of the process of its creation in time – are sufficient for the observation of the thermal hysteresis effect, whose hysteresis loop is reported. As the principle of superposition is demonstrated to be invalid in case of TSE, the thermal hysteresis curve converts in case of a continuous sweep in time into helical-type curve, for which the form and the magnitude of each cycle are slightly different as a result of the non-linear interaction of heat sources of the Universe through TSE. As a result of non-linear character of interaction of quantum objects with EM field (established theoretically by N. F. Ramsey and experimentally by P. Kusch), the self-ordering evolution process, observed for the thermal EM field, inevitably results in the same type of the evolution process in the whole energy spectrum of the EM radiation. The number of influence parameters in case of TSE is absolutely enormous, in confirmation of the previous theoretical studies of the cited paper of C. R. Stroud *et al.*

**Keywords:** surface energy, thermodynamic temperature, hysteresis, evolution process.

### **1. Introduction**

This communication we want to start with reminding of the theoretical prediction by Albert Einstein made in [1] that “classical thermodynamics can no longer be looked upon as applicable with precision...For the calculation of the free energy, the energy and the entropy of the boundary surface should also be considered”. The advancement of these ideas we find in [2a], where the thermal surface energy (TSE) is defined as the energy of boundary zones, located between the macroscopic parts of the system (sub-systems), in which the quasi-equilibrium thermal conditions are realized. It is stated in [2a] that the TSE is proportional to the area of contact between the two sub-systems, and that the internal energy of the system can be considered as additive, only when the value of the TSE can be regarded as negligible. It is clear that in case of experimental



demonstration of the TSE, the concept of thermodynamic temperature [2b] should be somehow modified and it should be, at least, in agreement with the notion of “temperature”, which is traditionally used in the J. Fourier thermal conduction theory [2c] and which definitely refers to thermal non-equilibrium conditions. Meanwhile, in accordance with A. Einstein requirements formulated in [3], thermodynamics can be applied only to isolated systems, and additionally, when all the transients in that system are terminated [3].

## 2. 2. Experiment.

The presented studies are based on the variation principle - one of the most general and powerful principles in experimental Physics. We have used a recently developed multi-channel synchronous detection technique (MSDT) [4a], which presents some modification of the famous R. Dicke’s method of synchronous detection. The specific feature of MSDT is that the modulation of the heat input to the system is realized through thermometer in one of the channels, and the detection is realized by several temperature sensors of the other channels [4a], which are located at different positions relative to the modulation source (Fig.1). In this case, the temperature information from the modulation channel can be used to find the synchronous temperature differences between the different points of the system, and, consequently, the propagation of the thermal signals can be precisely characterized both in time and in space.

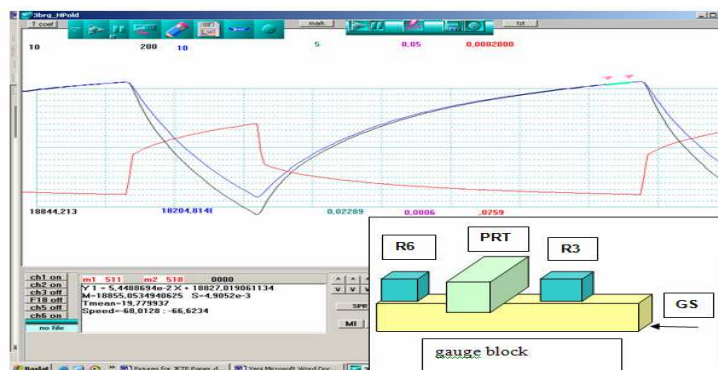


**Fig.1.** Simultaneous records of the resistance variations of the platinum resistance thermometer (PRT) and of two thermistors R6 and R3, located symmetrically relative to the PRT on the surface of the gauge block (as shown in the insert). During the current modulation cycle in the PRT, its current for  $\frac{1}{4}$  of the modulation period is kept at the level of 5mA and  $\frac{3}{4}$  of the period is kept at 1mA. The sensitivities of the thermistors are equal. In the insert, the location of one of the gauging surfaces is shown by the arrow.

A schematic outline of our experimental set-up and an example of unprocessed results of the measurements, performed on a homogeneous steel artifact, are presented in Fig.1. A steel (or tungsten carbide) gauge block (GB), with dimensions 9x35x100 mm, is located horizontally on three small-radius, polished spheres inside a closed Dewar. The Dewar is kept in a temperature



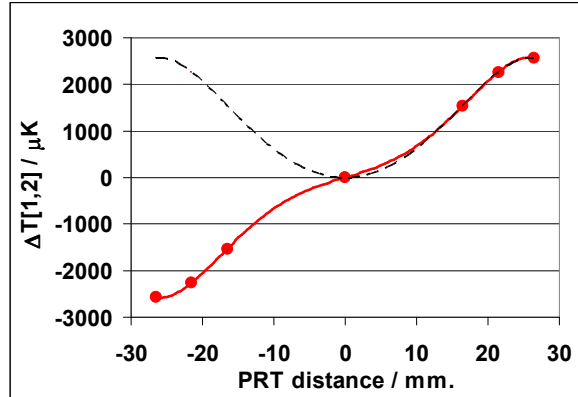


**Fig.3.** The dependence of the quantity  $\Delta T[1,2]$  (solid line) and the dependence of its absolute value (dashed line) as functions of the displacement of the PRT axis from the centre of the corresponding block surface.

By Fig.3, we show the dependence of the quantity  $\Delta T[1,2]$  on the displacement of the PRT axis relative to the centre of the corresponding block surface (see insert of Fig.1). The rapid decrease of the TSE amplitude with the increase of the R6 distance from the gauging surface, which can be approximated by the Gaussian curve, is clearly demonstrated. So, the term “surface energy” is quite appropriate in case of the TSE.

When combining the anti-symmetric dependence  $\Delta T[1,2]$  on the PRT displacement of Fig.3 with the much larger symmetric background of the induced temperatures, which is clearly observed in Fig.1 for large time intervals after the change of the modulation current, we come to the conclusion that *the total induced temperature variations (and consequently the total value of TSE), in the general case, are characterized by the lack of spatial symmetry.* The only exception is the singular point of the absolutely symmetric position of the PRT on the block surface.

The results of the experiment, which further clarifies the origin of TSE, are shown in Fig.4. Here, with very small uncertainty it is demonstrated that the magnitude of the quantity  $\Delta T[1,2]$  (and hence the magnitude of TSE) is linearly related to the increments in powers  $\delta P$ , delivered to the GB by the PRT. All the data points, presented in Fig.4, correspond to the values of the temperature differences  $\Delta T[1,2]$ , arising in the channels 1 and 2 exactly 13 minutes after the beginning of the heating period of the modulation cycle (see Fig.2). In Fig.4, we have two increments of the input power, corresponding to the PRT current increments from 1mA to 3mA and from 1mA to 5mA, respectively. These current variations in the modulation cycles were realized in two independent experiments, as well as the dependencies 1 and 2 also represent the results of the other two experiments, performed for the R6 separations from the nearest gauging surface  $L$ , equal to 4.5mm (dots) and 13.5mm (squares), respectively.

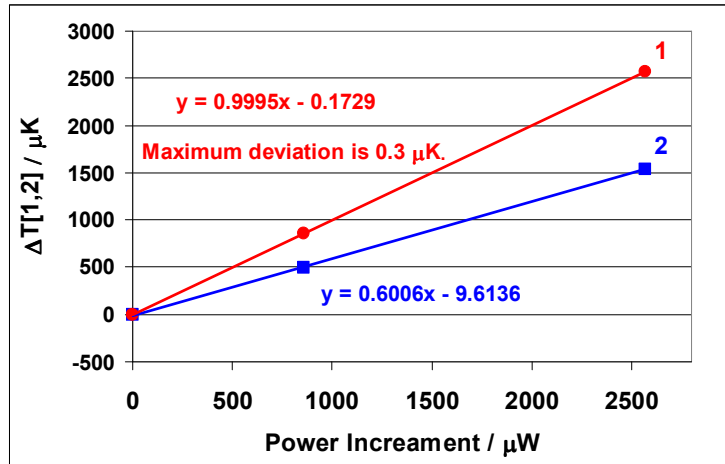


**Fig.4.** The effect of the PRT power increment on the quantity  $\Delta T[1,2]$ . Dependences 1 and 2 correspond to the separations of the R6 axis from the nearest gauging surface of  $L=4.5\text{mm}$  (dots) and  $L=13.5\text{mm}$  (squares), respectively. The decrease of the magnitude of the TSE with the increase of the R6 separation from the nearest gauging surface is clearly demonstrated by the dependences (1) and (2).

As it will be shown below, these experimental dependences establish a linear relations between the two vector quantities in our experiments: the Poynting vector  $\mathbf{S}$  of the external EM field, irradiating the surface of the block, and the vector quantity  $\Delta \mathbf{T}[1,2]$ , characterizing the difference between the induced temperature variations, observed in the channels 1 and 2. The ratio of the slopes of the dependencies 1 and 2, presented in the inserts of Fig.4, gives a precise value of the TSE decrease with the separation  $L$ . It is worth noting here, that as the process presents complicated functions of time and distances, the obtained value of the TSE decrease with distance is valid only for the indicated time.

To advance further in understanding the origin and properties of the TSE, we have performed another type of the differential temperature measurements. We study the vector quantity  $\Delta \mathbf{V}[1,2]$ , which characterize the difference in the induced temperature velocities, observed in the channels 1 and 2. This is easy to realize as the program in Fig.1 calculates both: the mean temperature in the channel for the specified time interval and the mean thermal velocity for the same period. The experimental points, shown in Fig.5 by dots, correspond to the heating period of the modulation cycle, while rhombi represent the cooling period. The reference points, corresponding to the last 30 minutes of the cooling period, are shown as squares. As the cooling period is chosen long enough, the difference between the measured velocities of the reference points in the channels is less than  $1\mu\text{K}/\text{min}$ . So, the linear fit to the reference points (shown in the insert of Fig.5) is practically equal to zero for all the presented time moments. As, the quantity  $\Delta \mathbf{V}[1,2]$  is defined by the difference between the induced values of the thermal velocities, the effect of the reference function on

the uncertainty of  $\Delta V[1,2]$  is negligible. Below it will be shown that  $\Delta V[1,2]$  describes the difference in the energy fluxes, entering (through boundaries) the unit volumes inside the artifact in the vicinities of the thermistors R6 and R3.

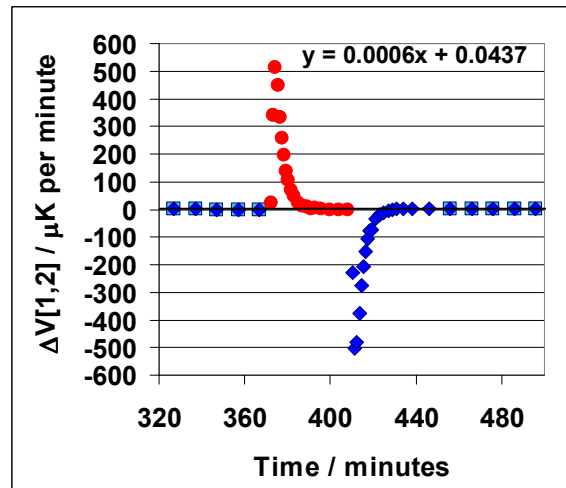


**Fig.5.** Variations in time of the difference between the induced temperature velocities, recorded by the channels 1 and 2,  $\Delta V[1,2]$ , that are observed during the heating period ( $I=5\text{mA}$ ) of the modulation cycle (dots) and during the cooling period ( $I=1\text{mA}$ ) of the modulation cycle (rhombi). These variations are measured relative to the reference points, shown as squares. The solid line shows the linear fit to the reference points, with the corresponding equation of the fit presented in the inset.

The plot, shown in Fig.5, indicates to the three key properties of the TSE, studied here. First, it shows that *the excessive energy flux does exist only during a short period of time after the change of the power value, dissipated in the PRT*. Second, *the magnitudes, the time scales and the forms of the curves are, practically, identical for the heating and for the cooling periods of the modulation cycle*. Third, *the direction of the propagation of the excessive energy flux is changed to the opposite during the heating and cooling periods of the cycle*. The latter follows immediately from the definition of the vector quantity  $\Delta V[1,2]$ , which keeps the information about the direction: its positive value corresponds to the excessive energy flux to the unit volumes in the vicinity of the gauging surface, while its negative value shows that the energy flux is larger to the unit volumes, located symmetrically relative to the PRT position in the direction of the bulk material. But in medium with absorption, the direction of the propagating energy defines the direction of the force, acting on the charged particles (free electrons) [2d, 6]. So, the dependence of Fig.5 shows that *the net systematic force on charged particles is present only during short moments of time at the beginning of the heating and cooling periods, and these forces have opposite signs, but approximately equal magnitudes and durations*. This observation shows the way how to present a hysteresis loop for the TSE, as in agreement with the standard procedure in the studies of ferromagnetic [2e] and ferroelectric [2f] materials, the X-axis variable should be related to the vector of force, acting on the

particles [2f]. The corresponding thermal hysteresis loop for the quantity  $\Delta T[1,2]$  is presented in Fig.6.

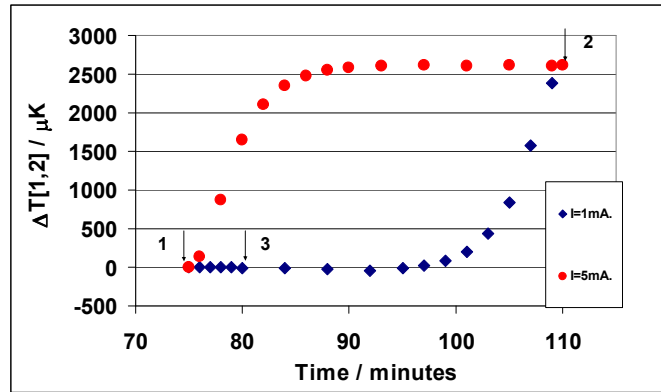


**Fig.6.** The thermal hysteresis loop for the quantity  $\Delta T[1,2]$ , corresponding to the temperature records of Figs. 1 and 2. The heating period of the cycle is shown by dots, while the cooling part is presented by rhombi. The time interval for the data points between arrows 1 and 3 is increased, as the temperature variations are negligible.

To obtain the form of the thermal hysteresis loop it is sufficient to present the data of Figs.1-2 not as a continuous sweep in time, but as a function of the direction of the external force (acting on the field-particle system inside the artifact) by inverting the time for the cooling period of the cycle. The corresponding plot is shown in Fig.6. Here, the induced temperature variations  $\Delta T[1,2]$  for the heating period are presented in the same time scale as in Fig.2. In Fig.6, the data points, corresponding the heating period are shown as dots (the beginning and the end of the heating are marked by two arrows 1 and 2). The data points for the cooling period of the cycle in Fig.6 are shown as rhombi. The corresponding path is indicated by arrows 2-3-1. Along this path the time variable is  $(111 - t)$ , which means the time inversion relative to the point  $t=111$  minutes, marked with arrow 2. Between the time interval, indicated by the arrows 2 and 3, the time scale is the same as in Fig.2. For the time interval between the arrows 3-1, where the variations of  $\Delta T[1,2]$  are negligible, the data points are presented for much larger time intervals, so that the end of the cooling period coincides with the beginning of the heating period. As the quantity  $\Delta T[1,2]$  is measured relative to the mean value of the several reference points at the very end of the cooling period of the cycle, we have a perfectly closed loop, only with some random jitter at a few  $\mu K$  level at the end parts of the loop that is absolutely negligible in comparison with the amplitude of the TSE effect.

*The energy, which is radiated by the system during the modulation cycle and which is responsible for heating the environment, is defined by the form of the thermal hysteresis curve. As for the other, well studied hysteresis effects:[4f], the TSE process is an irreversible one. To prove this, we can assume that the modulation of the current in the PRT is produced by a rechargeable battery and*

an electronic switch with negligible losses, and the state of the battery charge is continuously monitored by the device, which is used in all portable computers. We assume also that all the results of the measurements are recorded. Then for the normal play of the record we shall observe that the battery is gradually discharged, and the environment is heated by the energy, radiated by the gauge block. For the backward play of the record, we shall observe that for the purely periodic process, the energy of the battery is increased only as result of cooling of the thermal reservoir. But such process is strictly forbidden, as it contradicts the Clausius-Plank formulation of the second law of Thermodynamics (which presents the result of the analysis of a huge number of experimental facts and is known to have no exemptions) [2b]. So, in accordance with the Weyl idea how to check the symmetry in time of an arbitrary physical process, we are coming to the conclusion that the process of the build-up and of the disappearance of the surface thermal energy, presented by the experimental plots of Figs. 2 and 7, is definitely irreversible in time. Thus, *the thermal evolution process, described by the vector quantity  $\Delta T[1,2]$ , is irreversible in time and has no symmetry in space.*

Now we shall describe another important result of this study, which is closely related to the above mentioned properties of TSE. Experimental dependencies in the following figures show the effect of non-linearity of the material in the thermal evolution process, or, in other words, *the invalidity of the superposition principle for the external EM fields in the energy and momentum propagations inside the material artifact.* The main differences relative to the experiments of Figs.1-5 are the following. First, the separations between the adapters of the PRT and thermistors were increased from 10mm to 13.5mm, in order to study for steel and tungsten carbide blocks the effect of the heat source separation from the thermistor on the TSE amplitude. Second, two additional, auxiliary heat sources (resistors) were located inside the Dewar symmetrically and at the same distances from the gauging surfaces of the artifact. When one of them is switched on, the adjusted value of the dc current through this resistor produces a desired temperature difference between the locations of the thermistors R6 and R3. Thus in this experiment, the difference in the induced temperature variations, recorded by the channels 1 and 2, was measured when there was a systematic temperature difference on the artifact surface at the locations of the thermistors, belonging to the channels 1 and 2. The temperature difference between the channels,  $T[1,2]$ , shown as an additional parameter in Figs.7-8, was measured as a mean value of the temperature difference between the two thermistors, observed for the last 30 minutes of the cooling period of the modulation cycle. In Fig.7 the range of the variation of the parameter  $T[1,2]$  was between -2.46mK and 61.06mK.

As it clearly follows from Fig.7, the quantity  $\Delta T[1,2]$  is increasing with the increase of the temperature difference  $T[1,2]$ . The equation of the linear fit is presented in the insert. As the quantity  $\Delta T[1,2]$  corresponds to the difference in the temperature variations in the channels 1 and 2 that are induced by the increase of the current in the PRT and *this induced temperature difference is affected by the presence of the other heat source*, this means that the thermal

system is a nonlinear one, and *the superposition principle is not valid for the sources of external EM radiation in case of TSE.*

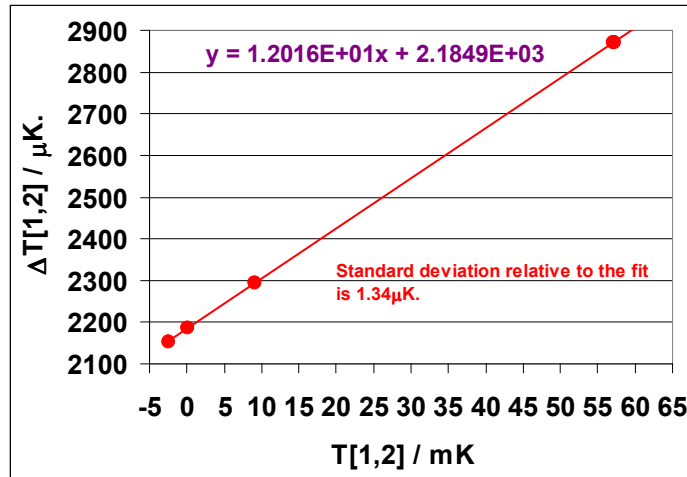


**Fig.7.** The dependence of the quantity  $\Delta T[1,2]$ , measured 13 minutes after the increase of the PRT modulation current in steel gauge block, on the temperature difference  $T[1,2]$  between the positions of the thermistors R6 and R3. (See text for other details).

To increase further the resolution of our measurements, the data points in Fig.7 present the averaged values of the quantity  $\Delta T[1,2]$ , obtained for several modulation cycles during the total duration of 5-7 hours. In this case, the abscissa values of the quantity  $T[1,2]$  correspond to the mean values of the temperature differences, obtained during the indicated measurement time. The mean thermal velocities, obtained during 5-7 hours of the measurements, were quite small, as these velocities correspond to the averaged values of temperature rates, obtained during several cycles of the temperature stabilization system in the laboratory. So, *the results of the measurements (shown in Fig.7) correspond to the quasi-static values of the temperature difference  $T[1,2]$ .*

As a consequence of the applied measurement procedure, the standard deviation, characterizing the scatter of the data points in Fig.7 relative to the linear fit, has been reduced to the value of  $1.32\mu K$ . Meanwhile, the total variation of the quantity  $\Delta T[1,2]$ , obtained for the shown range of temperature difference  $T[1,2]$  of  $63.5mK$ , exceeds the value of  $830\mu K$ . So, it follows from Fig.7 that the nonlinearity of the thermal system is not small at all (as the linear fit is  $1.2 \times 10^{-2}$ , when using the same units for both axes), and can be studied in detail when the temperature modulation technique is superimposed on a constant temperature bias.

Some results of the primary importance are illustrated by the plots of Fig.8, where we present the results for a tungsten carbide (TC) block in the presence of an external energy source, producing the energy flux in the same direction as the modulation source does during the heating period of the modulation cycle.

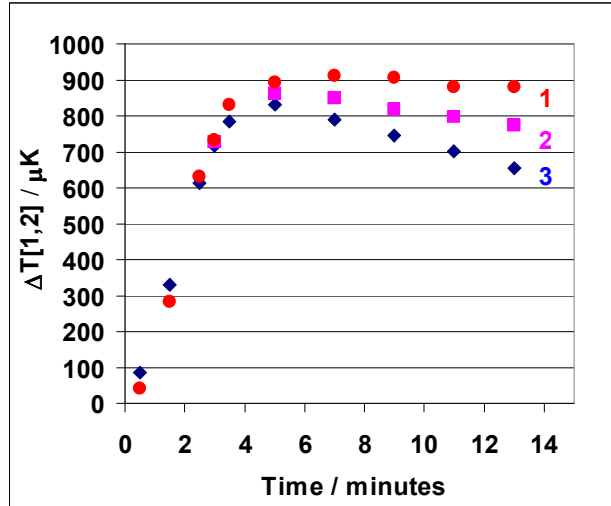


**Fig.8.** . The records of the quantity  $\Delta T[1,2]$ , that were obtained for the tungsten carbide block for the temperature differences between the channels  $T[1,2]$ , which were produced by an external heat source and which were equal to  $-1.72\text{mK}$  (dots);  $-7.2\text{mK}$  (squares) and  $-12\text{mK}$  (rhombi).

Here, we present the variations of the quantity  $\Delta T[1,2]$  as a function of time in the presence of an additional heat source, when the measurements were performed on a 100-mm TC block, when the separations between the PRT and thermistors adapters were 13mm (as in Fig.7). Comparison of the results for TC and steel blocks shows that the TSE process in TC block is found to be about 3 times faster than in the steel GB. So, even during the first 13 minutes after the increase of the modulation current in the PRT, a considerable part of the evolution process can be observed in case of the TC block.

The violation of the superposition principle in combination with hysteresis effect results in important consequences: *the presence of an additional heat source can change drastically the evolution process, which can be observed as a result of the energy modulation cycle inside the PRT at any point of the artifact.* This is illustrated in Fig.8, where we present the dependences  $\Delta T[1,2]$  versus time. Here, the dependences 1-3 (marked with dots, squares and rhombi) correspond to the mean values of the temperature differences between the channels  $T[1,2]$  equal to  $-1,17\text{mK}$ ,  $-8.2\text{mK}$  and  $-17.2\text{mK}$ , respectively. These values were measured for the reference points in three independent experiments, corresponding to three different power levels, dissipated by the auxiliary heat source.

As it is clearly demonstrated by the dependences 1-3, the additional heat source changes significantly the thermal evolution process. The maximum of the curve  $\Delta T[1,2]$  versus time, which can be detected in Fig.2 under close examination, now becomes clearly observed in Fig.8. The distinguishing features of the effect are variations of the maximum value of the dependences

$\Delta T[1,2]$  versus time, and the shift of the position of the maximum value on the time scale with the increase of the absolute value of the temperature difference  $T[1,2]$ . For example, for the dependences 1-3 the maximum values are equal to  $915\mu\text{K}$ ,  $863\mu\text{K}$  and  $846\mu\text{K}$ , respectively, when the uncertainty of these measurements is about  $2\text{-}5\mu\text{K}$ . With the increase of the value of the negative temperature difference  $T[1,2]$ , the position of the maximum value shifts to the smaller time intervals, elapsed after the increase of the modulation current in the PRT. For the dependences 1-3, the corresponding time intervals are, approximately, equal to 7.5, 5.45 and 4.15 minutes, respectively. Thus, we have presented a record of the evolution process, when *the external heat source changes the parameters and the dependence on time of the thermal evolution process*. For example, the difference between the dependences 1 and 3 in Fig.10 steadily increases with the increase of the time interval, and for the time intervals 3, 7 and 13 minutes after the increase of the modulation current, the differences between the dependencies 1 and 3 are equal to  $13\mu\text{K}$ ,  $123\mu\text{K}$  and  $255\mu\text{K}$ , respectively.

When analyzing the presented dependences of Fig.8 in the time interval between 0.5-1.5 minutes, we find a fascinating result. The auxiliary heat source, producing a stationary energy flux in the direction of the thermistor R6, is increasing the quantity  $\Delta T[1,2]$ , which describes the effect of the additional energy flux in the same direction, stimulated by the increase of the PRT modulation current (see Figs. 2 and 4). For this time interval we have, practically, a pure running wave of the propagating energy, as the reflection from the gauging surface is quite small. Indeed, the product of time interval of 1 minute and the value of the experimentally measured mean velocity of the energy propagation is less than the distance from the PRT to the gauging surface. Thus, it is demonstrated experimentally that when the energy reflection from the boundaries is negligible, *the energy flux, which is propagating in a homogeneous medium and which is induced by a step increase of the magnitude of the Poynting vector of the external EM field, is significantly increased, if the energy flux in the same direction has been created in advance by an auxiliary source of EM radiation*. This effect can be called as a thermal hysteresis effect for the running energy waves. As it follows from Fig.8, this effect can be of primary importance. For example, for the time interval  $t$  after the increase of the modulation current of 0.5 minute, the quantity  $\Delta T[1,2]$ , corresponding to the temperature bias  $T[1,2]$  of  $-17.2\text{mK}$ , exceeds by more than 2 times the quantity  $\Delta T[1,2]$ , observed for the bias of  $-1.2\text{mK}$ .

### 3. Conclusions and discussions.

First, we are to note here that the main parameters, affecting the indications of thermistors, are the energy and the Poynting vector of the external EM field, irradiating the surface of the thermometer. This field is produced by the motion of the charged particles and the EM field inside the artifact, which is in contact with the thermistors. As the charged particles in the artifact cannot tunnel through the gap of  $\sim 0.1\text{mm}$  (which is filled by nonconductive paste) between the thermistor adapter and the artifact, the only way for the energy transfer to

the adapter is through the absorption of EM field. This is the consequence of the Poynting's theorem of Electrodynamics [5], which says that the rate of change of the electromagnetic energy plus the total rate of doing work by the fields over the charged particles within the volume of a material artifact is equal to the flux of the Poynting vector,  $\mathbf{S}$ , entering the volume of the artifact through its boundary surface. The vector  $\mathbf{S}$  defines the energy current density inside a dielectric material with arbitrary level of losses [6], and the continuity equation for the total energy density,  $W$ , for the coupled field-particle system can be presented in the form (see eq.(2.17) in [6]):

$$\frac{\partial}{\partial t} W + m\Gamma \left( \frac{\partial}{\partial t} s \right)^2 = -\nabla \mathbf{S} \quad \dots(1).$$

Here,  $W$  presents the sum of the energy densities of the of the optical vibrational mode (kinetic and potential) and the energy density of the EM field;  $s$  is the relative spatial displacement field of two ions in the primitive unit cell;  $m$  is the reduced mass of two ions in the primitive unit cell, and  $\Gamma$  is the damping rate of the conversion of the optical mode into heat. The *rate of energy variations*, described by the first two terms in Eq. (1), is detected by thermistors and corresponds to the experimentally measured thermal velocity at the specified point of the material artifact. Thus, Eq. (1) establishes the linear relation between the total energy flux density  $\mathbf{S}$ , coming to the elementary volume through its boundary surface, and the thermal velocity, indicated by thermistor. So, the linear relation between the vector quantities  $\mathbf{S}$  and  $\Delta \mathbf{V}[1,2]$  is established (see Fig.3).

Under the approximations of [6], for a plane transverse EM wave, whose amplitude falls exponentially in  $z$ -direction, the cycled-averaged value of the total-energy current density in the  $z$ -direction  $\langle \mathbf{S}_z \rangle$  is related to the cycle-averaged energy density  $\langle W \rangle$  (see Eq. (2.19) in [6]) by a simple relation (4.16):

$$\langle \mathbf{S}_z \rangle = \mathbf{v}_e \langle W \rangle \quad \dots (2),$$

where  $\mathbf{v}_e$  is the velocity vector of the energy propagation in the material. Both parameters, velocity  $\mathbf{v}_e$  and the energy density  $W$ , can be precisely determined from our experimental data. So, the energy current density of a guided EM wave, which cannot be calculated theoretically (as constitutive relations for the medium are not known [5]), can be measured experimentally. This observation also refers to the cycle averaged value of the corresponding component of wave momentum density  $\langle G_z \rangle$ , which can be presented as the ratio of total-energy density  $\langle W \rangle$  and the value of the phase velocity  $v_p$ . As the cycle-averaged rate of the energy conversion into heat  $\langle R_H \rangle$  [6] is given by the ratio  $(\mathbf{v}_e \langle W \rangle / L)$ , (where  $L$  is the characteristic length of the decay of the field intensity), the TSE in the bulk material could have been predicted in [6].

Under the same approximations, in the one dimensional case, the total force density  $\langle \mathbf{F}_t \rangle$ , consisting of the Lorentz force density (which is acting on the particles) and of the time derivative of the EM field momentum density [6], can be presented by the expression:

$$\langle \mathbf{F}_z \rangle = [(1 + \eta^2 + \kappa^2) / (2\eta^2 L)] \langle W \rangle (\mathbf{v}_e / v_p) \dots (3).$$

Here,  $\eta$  is the refraction index of the medium and  $\kappa$  is the extinction coefficient. It follows from the equations presented above that for a specified material the force density  $\langle \mathbf{F}_z \rangle$  is linearly related to the rate of the energy dissipation  $\langle R_H \rangle$ . All the parameters in Eq. (3) can be measured quite accurately experimentally. Naturally, the force density  $\langle \mathbf{F}_z \rangle$  results in the systematic motion and in the displacement of free electrons. So, the mass transfer, as well as stresses and deformations, arising in the artifact as a result of the energy and momentum propagations in the medium, have to be taken into account in all adequate heat transfer theories.

It is also worth emphasizing here that our studies present an experimental confirmation of the main conclusions of the whole series of theoretical papers [7-9], started by R. H. Dicke and dealing with the interaction of the EM field with an ensemble of atoms or molecules. In accordance with [7, 8], the parameters of the spontaneous radiation process critically depend on the pre-history of the system and the type of its excitation. A simple example is presented in [7], showing that the system under consideration is anisotropic one: "As an example, consider a gas of two-level molecules, all excited", when "an intermolecular spacing is large compared with the radiation wavelength. Assume that a photon is emitted in the  $\mathbf{k}$  direction [7]". Then it follows from [7] that "the radiation probability in the direction  $\mathbf{k}$  has twice the probability (averaged over all other directions)" that "corresponds to the ordinary, incoherent spontaneous radiation of a single molecule". So, the system of molecules, interacting with the common EM field, is characterized by the angular correlation between the successively emitted photons [7].

In case of an arbitrary excitation level of the molecular system, when its dimensions are large in comparison with the wavelength of the resonant radiation, the coherent spontaneous decay of the system is still possible, but only in a single direction: "the polarization of the emitted or absorbed radiation is uniquely given by the direction of propagation" [7]. It is noted in [7]: "in the present case the incident radiation is assumed to be plane with the propagation vector  $\mathbf{k}$ , then after the excitation, the gas radiates coherently in the  $\mathbf{k}$  direction... Radiation in directions other than  $\mathbf{k}$  tends to destroy the coherence with respect to the direction  $\mathbf{k}$ ", as a consequence of the difference in the selection rules for coherent and incoherent spontaneous radiation (see equations (51) and (52) in [7]) ". So, the theoretical description of an ensemble of molecules, interacting with EM field, shows that the coupled field-particle system is the anisotropic one, and the considerations of space symmetry are not valid for this ensemble [7]. This is in strict agreement with our experimental results (see Figs.1-4).

As the systems, analyzed in [7, 8], are open ones, the process of the coherent spontaneous radiation is irreversible in time. When the molecules are in equivalent positions [8], the radiation process can be described by the motion of the super Bloch vector on the Bloch sphere, and the process stops when the total

dipole moment of the system acquires zero value [8]. In the general case of the initial excitation, some energy is still trapped in the system:” the system of atoms can no longer radiate coherently, and the remaining energy will be dissipated by whatever incoherent processes are available to the atoms” [8]. This property is also in agreement with our experiments, where the basic property of irreversible character of interaction with the external EM field of the ensemble of atoms in a metallic block immediately follows from the experimentally demonstrated thermal hysteresis loop.

On the other hand, our experimental demonstrations of the asymmetries in time and in space in case of thermal evolution process are in agreement with the more general violations of symmetries [10, 11], which have been predicted and explained theoretically by the prominent Russian physicist A. D. Sakharov in case of the physics of elementary particles (CPT asymmetries) [11]. Here, we can add that the irreversible character of the processes in Astronomy has been established since 1927, when the British astronomer Arthur Eddington introduced the concept of the “arrow of time” - the distinguished direction of the time, which can be determined by the study of organizations of material objects in the Universe. The numerous studies of the Universe performed with radio-telescopes have demonstrated clearly its anisotropy and the lack of spatial symmetry [12]. One of the first experimental observations of the violation of the reflection symmetry in the physics of elementary particles was performed using  $\beta$ -disintegration of radioactive isotope of cobalt in strong magnetic fields at low temperatures [13]. Numerous biological studies [14, 13] confirm unambiguously that the asymmetries in time and in space are the fundamental properties of Nature.

Specially, it should be emphasized that the fundamental result of [8], dealing with enormous number of influence parameters in the interaction of EM field with an ensemble of atoms, have been experimentally confirmed by these studies. It follows from [8] that in calculation of the field, emitted by the ensemble, all the distances between the atoms, the mutual orientations of the dipole moments and the levels of the initial excitations of all atoms are the necessary parameters in this procedure. So, the number of influence parameters increases dramatically with the increase of the number of atoms in the ensemble. In case of interaction of macroscopic objects through the EM field the number influence parameters are further increased, as additional information about the forms, properties of the materials and mutual solid angles of the observations has to be included into the influence parameters even in free space. For the experiments on Earth, when the energy from Sun is propagating through the turbulent atmosphere, the number of parameters is infinite [2a]. The well-established irregularities of the Earth rotation, convert the curves of Fig.1 into spirals, with slightly different adjacent cycles, as a result of the time asymmetry in the process of the energy propagation from the Sun. Naturally, *the thermal evolution process, which is described by the infinite number of parameters, has the infinite number of the modes of existence*, and this observation is in agreement with one of the fundamentals of the Ancient Indian philosophy.

## Acknowledgements.

The authors gratefully acknowledge financial support of our studies at INMETRO by the National Research Council (CNPq) of Brazil. The technical and moral support of our studies by the staff of INMETRO is highly appreciated. The authors are grateful to the staff of the Physical department of the Yeditepe University (Turkey) for the support and useful discussions.

## References

1. A. Einstein, *Investigations on the Theory of the Brownian Motion*, Annalen der Physik, v. 17, pp.549-566, (1905).
2. D. V. Sivukhin, *General Course of Physics*, Physmatlit, Mscow, (2008)  
**V2**, *Thermodynamics*, pp.44-71 [2a]; **V2**, pp.85-110 [2b]; **V2**, pp.162-182 [2c];  
**V.4**, *Optics*, pp. 466-480 [2d];  
**V3**, *Electricity*, pp.293-317 [2e]; **V3**, pp. 159-172 [2f].
3. A. Einstein, *A Theory of the Foundations of Thermodynamics*, Annalen der Physik, **11**, pp.170-187 (1903).
4. A. Titov, I. Malinovsky, *Nanometrology and high-precision temperature measurements under varying in time temperature conditions*, **Proc. SPIE**, **5879**, ed by J. E. Decker and Gwo-Sheng Peng, 587902-01 – 587902-11 (2005) [4a];  
*New techniques and advances in high-precision temperature measurements of material artefacts*, Can. J. of Scientific and Ind. Research, **V.2**, No.2, pp. 59-81 (2011) [4b];  
A. Titov, *et al*, *Precise certification of the temperature measuring system of the original Kősters interferometer and ways of its improvement*, **Proc. SPIE** **5879**, ed by J. E. Decker and Gwo-Sheng Peng, 587904-01 – 587904-11 (2005) [4c].
5. J. D. Jackson, *Classical Electrodynamics*, J. Willey and Sons, 3-ed, pp.259-262 (1999).
6. R. Loudon, L. Allen and D. F. Nelson, *Propagation of electromagnetic energy and momentum through an absorbing dielectric*, Phys. Rev. E, **55**, 1071-1085 (1997).
7. R. H. Dicke, *Coherence in Spontaneous Radiation Processes*, Phys. Rev. **93**, pp. 99-110 (1954).
8. C. R. Stroud, *et al*, *Superradiant Effects in Systems of Two-Level Atoms*, Phys. Rev. A, **5**, pp. 1094-1104 (1972).
9. F. W. Cummings and Ali Dorri, *Exact Solution for spontaneous emission in the presence of N atoms*, Phys. Rev. A, **28**, pp.2282-2285 (1982).
10. A. D. Sakharov, *Violation of CP Symmetry, C-Asymmetry and Baryon Asymmetry of the Universe*, JETP Lett. **5**, pp.24-27 (1967).
11. A. D. Sakharov, *Topological structure of elementary particles and CPT asymmetry*, in "Problems in theoretical physics", dedicated to the memory of I. E. Tamm: Nauka, Moscow, pp.243-247, (1972).
12. G. Smoot, M. Gorenstein, and R. A. Muller, *Detection of anisotropy in the cosmic blackbody radiation*, Phys. Rev. Let. **39**, 898 (1977).
13. R. P. Feynman, R. B. Leighton and M. Sands, *The Feynman Lectures on Physics*, Addison-Wesley, 1-ed, **V.3**, Ch.52, pp.1-12 (1964).
14. Ch. Darwin and A. R. Wallace, *On the Tendencies of Species to Form Varieties, and the Perpetuation of Varieties and Species by Natural Means of Selection*, Journal of the Proceedings of Linnean Society of London, Zoology 3, **3** (9), pp.46-50 (1858).